ESC European Society of Cardiology

Cardiovascular Research (2021) **117**, 472–483
doi:10.1093/cvr/cvaa036

NOS1AP polymorphisms reduce NOS1 activity and interact with prolonged repolarization in arrhythmogenesis

Carlotta Ronchi [1†], Joyce Bernardi [1†], Manuela Mura[2†], Manuela Stefanello[2], Beatrice Badone [1], Marcella Rocchetti [1], Lia Crotti[3,4,5], Paul Brink[6], Peter J. Schwartz [3], Massimiliano Gnecchi [2,7,8*‡], and Antonio Zaza [1,9*‡]

[1]Department of Biotechnology and Biosciences, University of Milano-Bicocca, Piazza della Scienza 2, 2016 Milano, Italy;[2] Department of Cardiothoracic and Vascular Sciences, Fondazione IRCCS Policlinico San Matteo - Laboratory of Experimental Cardiology for Cell and Molecular Therapies, Viale Camillo Golgi 19, 27100 Pavia, Italy;[3] Center for Cardiac Arrhythmias of Genetic Origin, IRCCS Istituto Auxologico Italiano, Via Pier Lombardo 22, 20135 Milan, Italy;[4]Department of Medicine and Surgery, University of Milano-Bicocca, Milano, Italy;[5]Department of Cardiovascular, Neural and Metabolic Sciences, IRCCS Istituto Auxologico Italiano, San Luca Hospital, Milan, Italy;[6]Department of Medicine, University of Stellenbosch, Tygerberg, South Africa;[7]Unit of Cardiology, Department of Molecular Medicine, University of Pavia, Pavia, Italy;[8]Department of Medicine, University of Cape Town, Cape Town, South Africa; and [9]Cardiovascular Research Institute (CARIM), Maastricht University, Maastricht, Netherlands

Received 28 January 2019; revised 28 October 2019; editorial decision 31 January 2020; accepted 10 February 2020; online publish-ahead-of-print 15 February 2020

Time for primary review: 27 days

Aims *NOS1AP* single-nucleotide polymorphisms (SNPs) correlate with QT prolongation and cardiac sudden death in patients affected by long QT syndrome type 1 (LQT1). NOS1AP targets NOS1 to intracellular effectors. We hypothesize that *NOS1AP* SNPs cause NOS1 dysfunction and this may converge with prolonged action-potential duration (APD) to facilitate arrhythmias. Here we test (i) the effects of NOS1 inhibition and their interaction with prolonged APD in a guinea pig cardiomyocyte (GP-CMs) LQT1 model; (ii) whether pluripotent stem cell-derived cardiomyocytes (hiPSC-CMs) from LQT1 patients differing for *NOS1AP* variants and mutation penetrance display a phenotype compatible with NOS1 deficiency.

Methods and results In GP-CMs, NOS1 was inhibited by S-Methyl-L-thiocitrulline acetate (SMTC) or Vinyl-L-NIO hydrochloride (L-VNIO); LQT1 was mimicked by I_{Ks} blockade (JNJ303) and β-adrenergic stimulation (isoproterenol). hiPSC-CMs were obtained from symptomatic (S) and asymptomatic (AS) *KCNQ1*-A341V carriers, harbouring the minor and major alleles of *NOS1AP* SNPs (rs16847548 and rs4657139), respectively. In GP-CMs, NOS1 inhibition prolonged APD, enhanced I_{CaL} and I_{NaL}, slowed Ca^{2+} decay, and induced delayed afterdepolarizations. Under action-potential clamp, switching to shorter APD suppressed 'transient inward current' events induced by NOS1 inhibition and reduced cytosolic Ca^{2+}. In S (vs. AS) hiPSC-CMs, APD was longer and I_{CaL} larger; NOS1AP and NOS1 expression and co-localization were decreased.

Conclusion The minor *NOS1AP* alleles are associated with NOS1 loss of function. The latter likely contributes to APD prolongation in LQT1 and converges with it to perturb Ca^{2+} handling. This establishes a mechanistic link between *NOS1AP* SNPs and aggravation of the arrhythmia phenotype in prolonged repolarization syndromes.

* Corresponding authors. Tel: +39 02 6448 3307, E-mail: antonio.zaza@unimib.it (A.Z.); Tel: +39 0382 982107; fax: +39 0382 502481, E-mail: m.gnecchi@unipv.it (M.G.)

† These authors contributed equally as first authors to the article.

‡ These authors contributed equally as senior authors to the article.

Published on behalf of the European Society of Cardiology. All rights reserved. © The Author(s) 2020. For permissions, please email: journals.permissions@oup.com.

Graphical Abstract

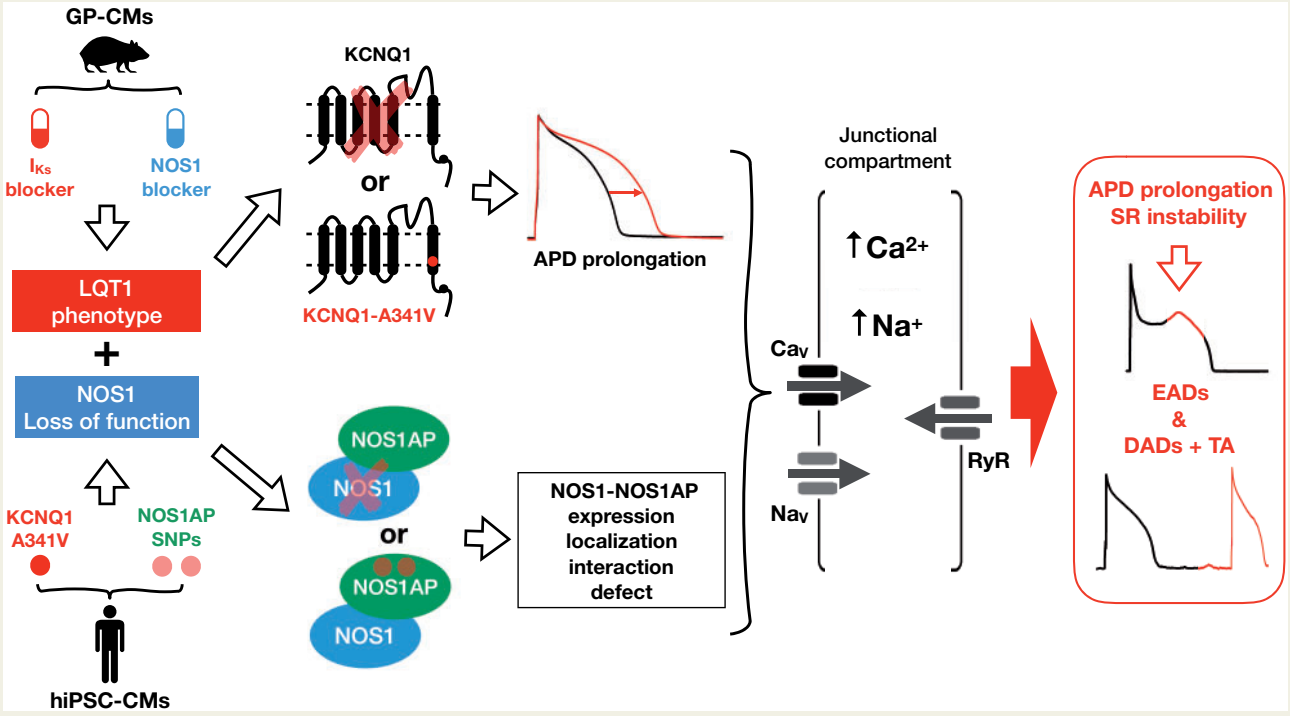

Keywords • LQT1 • NOS1AP polymorphism • NOS1 defect • hiPSC-derived cardiomyocytes • Arrhythmias

1. Introduction

The 'neuronal' isoform of NO-synthase (NOS1 or nNOS) is expressed in cardiomyocytes (CMs) and localized to a subcellular compartment relevant to Ca^{2+} handling by an 'anchoring protein' named NOS1AP,[1] which may be crucial in targeting NOS1 signal. As expected from its localization, NOS1 activity modulates L type Ca^{2+} current (I_{CaL}),[2,3] ryanodine receptor 2 (RyR2),[4] and SERCA2a,[5,6] thus contributing to sarcoplasmic reticulum (SR) stability.

Single-nucleotide polymorphisms (SNPs) on the *NOS1AP* gene are associated with QT prolongation in the general population[7] and to increased incidence of sudden death in patients affected by long QT syndrome type 1 (LQT1).[8,9] This leads to hypothesize that NOS1 signalling may differ among *NOS1AP* variants, thus acting as an arrhythmogenic co-factor in the setting of action-potential duration (APD) prolongation. If so, the well-known variable penetrance of LQTS mutations and the inadequacy of QT interval in predicting arrhythmic events in acquired LQTS[10] might reflect *NOS1AP* polymorphism.

We tested this hypothesis by (i) evaluating the effects of concurrent NOS1 modulation and APD prolongation in mature guinea-pig (GP) ventricular cardiomyocytes (GP-CMs), with focus on SR stability; (ii) comparing them to the phenotype of human CMs (hiPSC-CMs) derived from carriers of a malignant LQT1 mutation but presenting distinct mutation penetrance and expressing different *NOS1AP* variants[11,12]; and (iii) relating *NOS1AP* variants to the expression and localization of NOS1 and NOS1AP proteins.

2. Methods

A detailed description of material and methods is provided in the Supplementary material online.

2.1 Patients

Out of a South African (SA) founder population thoroughly characterized by our group,[11,12] we selected two patients, carriers of the KCNQ1-A341V mutation and of different *NOS1AP* SNPs, as representative cases of asymptomatic (AS) and highly symptomatic (S) LQT1 phenotypes. Two additional subjects were enrolled as carriers of minor and major *NOS1AP* variants, respectively, but on a background of normal (WT) *KCNQ1* genotype. All patients were enrolled in the study after signing informed consent. The study was approved by the Health Research Ethics Committee of the University of Stellenbosch (nr. N13/01/002) and by the ethics committee of the Fondazione IRCCS Policlinico San Matteo, Pavia. The investigation conforms to the principles outlined in the Declaration of Helsinki. Clinical characteristics of S and AS carriers are summarized in the Supplementary material online, *Table S1*.

2.2 Experimental models

The experiments were carried out on isolated GP-CMs ventricular myocytes and hiPSC-CMs. GPs were euthanized by cervical dislocation under anaesthesia with zolazepam + tiletamine (Telazol 100 mg/kg i.p.) All experiments involving animals (methods detailed in the Supplementary

material online) conformed to the guidelines for Animal Care endorsed by the University of Milano-Bicocca and to the Directive 2010/63/EU of the European Parliament on the protection of animals used for scientific purposes.

hiPSC-CMs were differentiated from hiPSCs lines previously generated and characterized by our group,[13,14] and derived from one S and one AS KCNQ1-A341V heterozygous mutation carriers, genotyped for the mutation and *NOS1AP* single nucleotide variants (SNPs):

- S hiPSC-CMs carried the minor variants rs16847548 and rs4657139 in homozygosis.
- AS hiPSC-CMs carried the major alleles of the respective positions.

hiPSC-CMs were also obtained from two healthy donors (wildtype for *KCNQ1*): one heterozygous for the minor *NOS1AP* variant rs16847548 (belonging to the SA population), the other carrying the major variants of all alleles (not belonging to the SA population). Results concerning the healthy donors are presented in the Supplementary material online.

The generation and molecular characterization of hiPSC-CMs were carried out using a protocol previously published[13,14] and described in the Supplementary material online.

2.3 Electrophysiology

Electrophysiological measurements, performed in GP-CMs and hiPSC-CMs, included I-clamp recordings, aimed at testing the phenotype and the effect of interventions on the electrical activity, and V-clamp recordings. Standard V-clamp protocols were used for evaluating I_{CaL}, I_{Ks}, and I_{Kr}; I_{NaL} was measured as the TTX-sensitive current during the AP plateau phase in action-potential clamp (AP clamp) experiments. AP clamp was also used to test the role of APD prolongation in facilitating 'transient inward current' (I_{TI}) events, reflective of SR instability.

All measurements were performed in the whole-cell configuration at physiological temperature (36°C). Details on the recording solutions and signal acquisition for all protocols are provided in the Supplementary material online.

2.4 Intracellular Ca^{2+} recordings

Cytosolic Ca^{2+} was optically measured in cardiomyocytes loaded with 10 μM Fluo4-AM. Ca^{2+} signals (expressed in normalized units F/F_0) were evaluated as the amplitude of V-induced Ca^{2+} transient (Ca_T), diastolic Ca^{2+} (Ca_D), and caffeine-induced Ca^{2+} release (to measure SR Ca^{2+} content, Ca_{SR}). The recordings were performed under control and NOS1 inhibition (by SMTC) in GP-CMs and AS hiPSC-CMs. Details on intracellular Ca^{2+} measurements are provided in the Supplementary material online.

2.5 Molecular studies

Transcript and protein expression were measured by RT-PCR and western blot, respectively. Protein expression and localization were detected by immunofluorescence; co-localization was assessed with the Duolink Proximity Ligation Assay (PLA) (Sigma Aldrich).

2.6 Chemicals

NOS1 was inhibited by SMTC (3 μM, Caymal Chemical)[15] or by L-VNIO (Caymal Chemical, data in the Supplementary material online).[5] I_{Ks}, I_{Kr}, and I_{CaL} were blocked by JNJ303 (2 μM, Tocris Bioscience), E-4031 (5 μM, Alomone Labs), and nifedipine (5 μM, Sigma), respectively. I_{NaL} was blocked by TTX (1 μM, Tocris Bioscience). Dimethyl sulphoxide (DMSO) and ethanol were used as solvents; their final concentration did not exceed 0.1%. All other chemicals were purchased from Sigma.

2.7 Statistical analysis

The Student's paired or unpaired *t*-test was applied as appropriate to test for significance between means. Difference between percentages was tested by the χ^2 analysis applied to raw numbers. Average data are expressed and plotted as mean ± standard error of the mean. Statistical significance was defined as $P < 0.05$ (NS, not significant). Sample size (*n*/*N*, number of cells/number of animals or differentiations) is specified for each experimental condition in the respective figure legend.

3. Results

3.1 Studies in guinea pig cardiomyocytes

3.1.1 Effect of NOS1 inhibition on repolarization and occurrence of arrhythmogenic events

This set of experiments aimed at testing the effect of NOS1 inhibition on repolarization (APD_{90}) and afterdepolarizations in basal conditions and when simulating the arrhythmogenic setting of LQT1 (ISO-induced β-adrenergic stimulation plus I_{Ks} blockade by JNJ).[16,17] To this end, the effect of SMTC was tested before (basal) and during ISO + JNJ (LQT1 setting).

Under basal conditions, NOS1 inhibition markedly prolonged APD_{90} (*Figure* 1*A* and *B*). I_{Ks} blockade prolonged APD_{90} only slightly and by a similar percent in CTRL and when NOS1 was inhibited (*Figure* 1*C*), thus suggesting that NOS1 inhibition did not interfere with I_{Ks} channel activity. The superimposition of β-adrenergic stimulation further prolonged APD_{90} and this prolongation was significantly larger when NOS1 was inhibited (39.7 ± 5.1% vs. 24.2 ± 4.0%, $P < 0.05$. *Figure* 1*D*).

Under basal conditions, delayed afterdepolarizations (DADs) occurred neither in CTRL nor during NOS1 inhibition. In the presence of I_{Ks} blockade, ISO 1 nM induced DADs in 22% of GP-CMs in the CTRL group; ISO effect was enhanced by NOS1 inhibition (DADs in 93% vs. 22%; $P < 0.01$) (*Figure* 1*E*). Moreover, the time interval between the beginning of ISO perfusion and the appearance of DADs was significantly shortened by NOS1 inhibition (*Figure* 1*F*). Triggered activity could be induced during NOS1 inhibition by 10 nM ISO (*Figure* 1*G*). Possibly due to the relatively high pacing rate, EADs were never observed in GP-CMs.

To rule out that these observations resulted from SMTC effect other than NOS1 inhibition (ancillary effects), experiments were repeated using a different NOS1 inhibitor, L-VNIO. The results obtained with L-VNIO, detailed in the Supplementary material online *Figure S1*, were comparable to those observed in the presence of SMTC, thus indicating that the effect of these agents truly reflects NOS1 inhibition.

To summarize, NOS1 inhibition significantly prolonged APD_{90} under basal condition, it did not change the effect of I_{Ks} blockade, but it almost doubled the prolonging effect of superimposed ISO. NOS1 inhibition also facilitated induction of afterdepolarizations by ISO.

3.1.2 Effect of NOS1 inhibition on currents contributing to repolarization

The aim of these experiments was to test the effect of NOS1 inhibition on the membrane currents more likely to account for its effect on repolarization (above). These include the inward components I_{CaL} and I_{NaL} and the outward ones I_{Kr} and I_{Ks}.

Peak I_{CaL} density was enhanced by NOS1 inhibition (*Figure* 2*A* and *B*) due to a 20.7 ± 0.4% increase in maximal conductance (g_{max}) (Supplementary material online, *Table S2*). I_{CaL} steady-state activation and inactivation parameters, 'window' current amplitude and inactivation

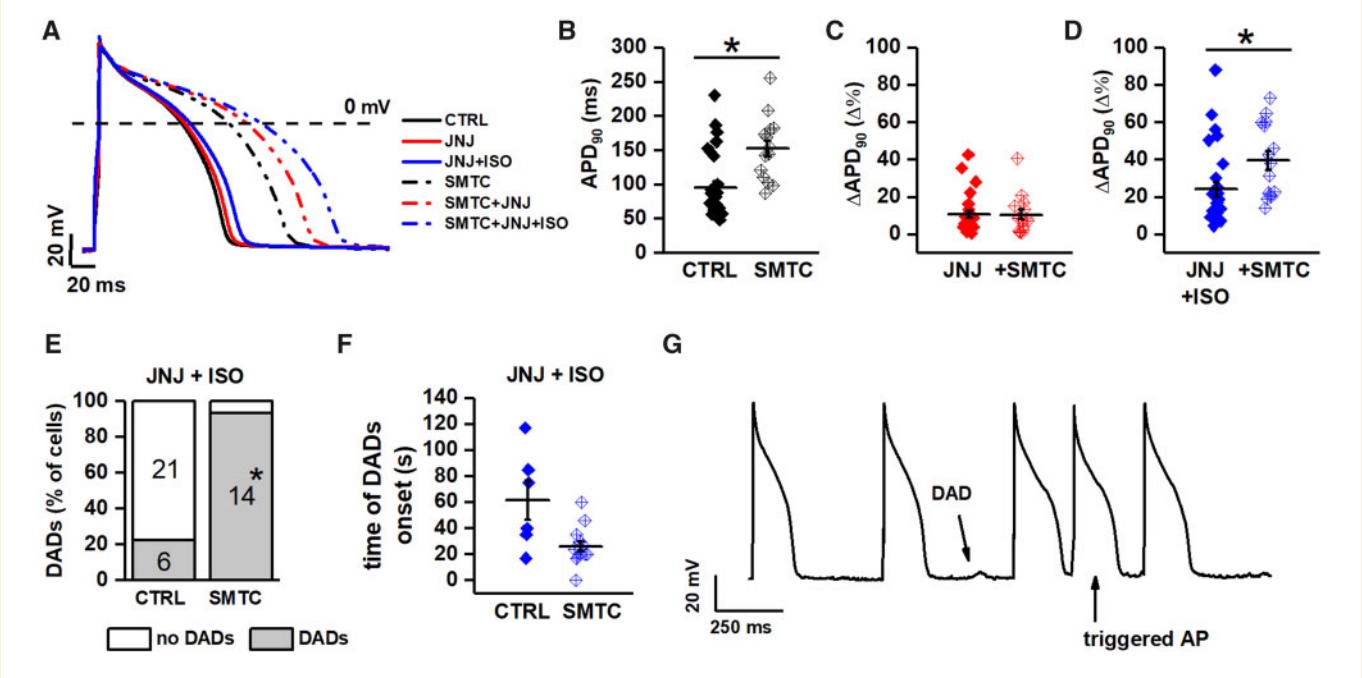

Figure 1 Effect of NOS1 inhibition on APD and DADs in GP cardiomyocytes. (*A*) representative APs from control (CTRL, solid lines) and NOS1 inhibition (SMTC, dotted lines); colour code: black = basal, red = I_{Ks} blockade alone, and blue = plus 1 nM ISO. (*B*) Effect of NOS1 inhibition on APD_{90} in basal condition. (*C*) Percent change (Δ%) in APD_{90} resulting from I_{Ks} blockade in CTRL and during NOS1 inhibition. (*D*) Same as in C after adding ISO. (*E*) Effect of NOS1 inhibition on DADs incidence (at 1 nM ISO). (*F*) Effect of NOS1 inhibition on the time of DADs onset after the beginning of ISO challenge. (*G*) Example of triggered activity observed during strong β-adrenergic stimulation in the presence of NOS1 inhibition (L-VNIO + 10 nM ISO). Sample sizes: CTRL $n = 27/12$ and SMTC $n = 15/4$ for *B–E*; CTRL $n = 6/5$ and SMTC $n = 14/4$ for *F*. $^*P < 0.05$ vs. control from unpaired Student's *t*-test and the χ^2 test as appropriate.

rate were unaffected (*Figure 2C* and Supplementary material online, *Table S2*). SMTC markedly enhanced TTX-sensitive current during the AP plateau phase (*Figure 2D–F*); I_{TTX} increment was maximal around +20 mV (*Figure 2E*), a membrane potential compatible with an increment of I_{NaL} as opposed to 'window I_{Na}'.

The outward components of repolarizing current (I_{Kr} and I_{Ks}) were marginally affected by NOS1 inhibition, a slight slowing of I_{Ks} activation being the only significant effect. Details on I_{Kr} and I_{Ks} modulation are provided in the Supplementary material online, *Figures S2* and *S3*.

3.1.3 Effect of NOS1 inhibition on intracellular Ca^{2+} dynamics

The above observations indicate that NOS1 inhibition *per se* results in SR instability (increased DADs incidence), likely favoured by intracellular Ca^{2+} overload. We then investigated the effect of NOS1 inhibition (by SMTC) in the presence of ISO (1 nM) on intracellular Ca^{2+} dynamics. Altogether, the results obtained are consistent with I_{CaL} enhancement, increased Ca^{2+} leak from the SR and facilitation of spontaneous Ca^{2+} release (SCR) (see Supplementary material online, *Figure S4*). However, the magnitude of SMTC-induced changes, albeit statistically significant for some of the parameters, was smaller than expected. Moreover, in contrast to their electrical counterpart (DADs or I_{TI}), SCR events were observed with a surprisingly low frequency and in un-patched cells only (Supplementary material online, *Figure S4G*). This is likely to represent an artefact originated from the experimental conditions required for Ca^{2+} recordings (see Section 4). Accordingly, the results concerning the effect of NOS1 inhibition on intracellular Ca^{2+} should be regarded as 'quantitatively inaccurate' (underestimation) and are reported in detail in the Supplementary material online.

3.1.4 Convergence of reduced NOS1 activity and slow repolarization in affecting I_{TI} occurrence and Ca^{2+} loading

According to the working hypothesis, APD prolongation may amplify the effect of NOS1 inhibition on SR instability from an AS condition into an arrhythmogenic one. We tested this hypothesis by evaluating the effect of changing APD (under AP-clamp conditions, in the presence of 1 nM ISO) on membrane current events (I_{TI}) indicative of SR instability (*Figure 3A*).

In CTRL, I_{TI} occurred in 68.7% of GP-CMs during the long AP; this incidence was not significantly affected by NOS1 inhibition (*Figure 3B*). The charge flowing during individual I_{TI} events, reflecting the magnitude of SCR, was also not affected by NOS1 inhibition (31.4 ± 4.9 vs. 37.91 ± 10.6 fC/pF, NS). Nevertheless, whereas all CTRL GP-CMs displayed only single I_{TI} events, up to two sequential I_{TI} events were detected in 30% of GP-CMs during NOS1 inhibition ($P < 0.05$ vs. CTRL; *Figure 3C*). In cells consistently displaying I_{TI} events with the long AP, switching to the shorter APD suppressed I_{TI} in 81.8% and 100% of GP-CMs in CTRL and NOS1 inhibition, respectively (*Figure 3D*); likely because the suppression rate observed in control conditions was already close to 100%, the effect of NOS1 inhibition only approached significance ($P = 0.06$).

These results confirm that APD prolongation is a factor in the genesis of SCR events; we hypothesized that this is the consequence of changes in intracellular Ca^{2+} loading. To test this hypothesis, we performed the same AP-clamp experiments described above (long to short AP in the

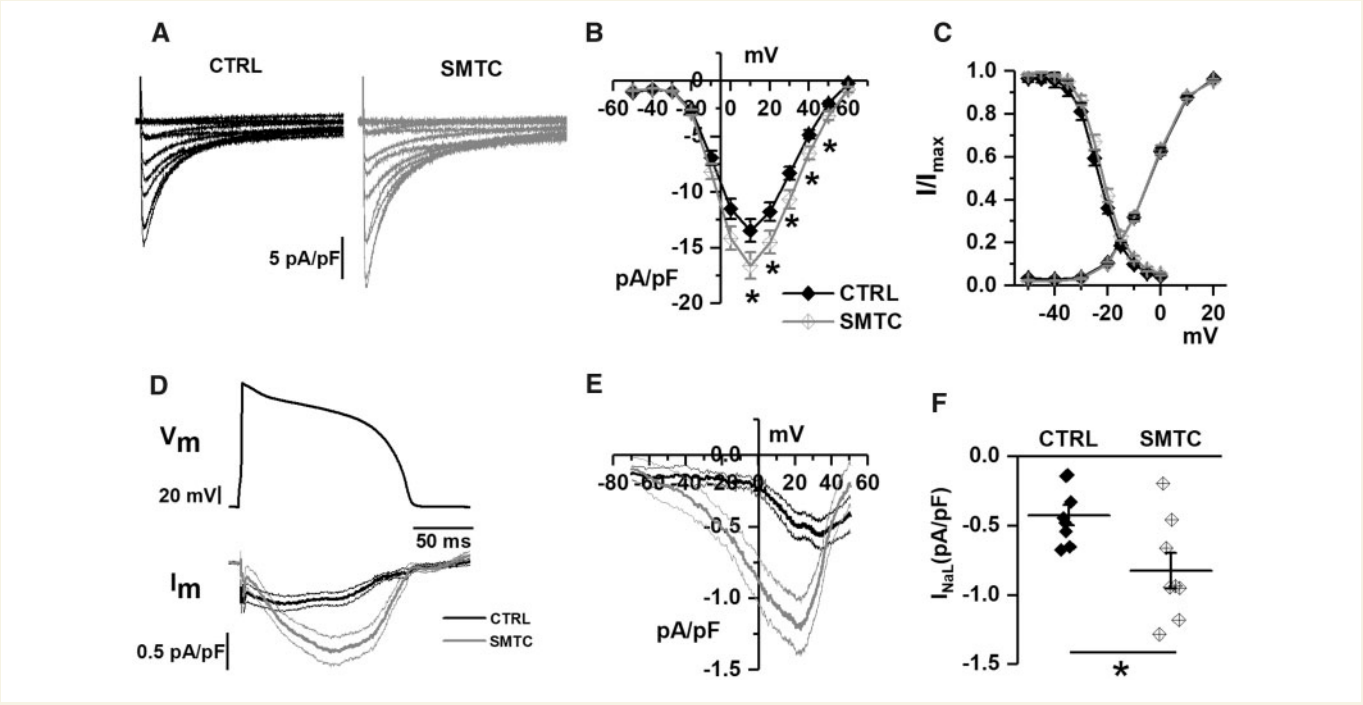

Figure 2 Effect of NOS1 inhibition on I_{CaL} and I_{NaL} in GP cardiomyocytes. (*A*) Representative I_{CaL} recordings at different voltages in control (CTRL) and during NOS1 inhibition (SMTC); (*B*) average (±SE) I/V relationships of peak I_{CaL} density in CTRL and during NOS1 inhibition; (*C*) average steady-state activation and inactivation curves in CTRL and NOS1 inhibition. (*D*) Long AP waveform (top) and average traces of I_{NaL} (bottom). (*E*) Dynamic I/V relationship of traces shown in *D*. (*F*) TTX-sensitive current (I_{NaL}) in control and under NOS1 inhibition. Sample sizes: CTRL n = 25/4 and SMTC n = 20/3 for *A–C* panels; CTRL n = 8/2 and SMTC n = 8/2 for *D–F* panels. *P < 0.05 vs. CTRL from two-way ANOVA for repeated measurements.

presence of ISO 1 nM) while measuring diastolic Ca^{2+} (Ca_D) and Ca^{2+} transient amplitude (Ca_T) (*Figure 4A*). APD shortening reduced both Ca_D and Ca_T; while the effect on Ca_D was reversible, the one on Ca_T was not (*Figure 4B*), possibly due to I_{CaL} run-down during the long recording period.

Under AP clamp, NOS1 inhibition significantly prolonged the $t_{1/2}$ of Ca^{2+} decay during the transient (*Figure 4C*) but affected neither Ca_D and Ca_T, nor their changes upon APD shortening (*Figure 4D*).

To rule out dependency of intracellular Ca^{2+} parameters on the waveforms sequence, the latter was inverted in a subset of experiments. Irrespective of the waveform sequence, Ca_D was consistently higher under the longer AP; as above, the response of Ca_T was less consistent, in a way again compatible with I_{CaL} run-down (Supplementary material online, *Figure S5*). In contrast to the high incidence of DADs and I_{TI} events (in I-clamp and AP-clamp experiments, respectively), SCR events were not observed under AP clamp in Fluo4-AM loaded GP-CMs.

Thus, facilitation of I_{TI} occurrence by AP prolongation was associated with changes in Ca^{2+} dynamics compatible with an increased intracellular Ca^{2+} load. NOS1 inhibition increased the occurrence of multiple I_{TI} events and slowed SR Ca^{2+} reuptake. During NOS1 inhibition AP shortening suppressed I_{TI} in all cardiomyocytes; under control conditions, I_{TI} suppression by AP shortening was less consistent but still frequent.

3.2 Studies in KvLQT1-mutant hiPSC-CMs

The aims of these experiments were (i) to compare the functional phenotype of hiPSC-CMs derived from S and AS LQT1 patients and check, whether differences compatible with the effects of NOS1 inhibition in GP-CMs were detectable; (ii) to test whether in hiPSC-CMs the S status (minor *NOS1AP* allele) was associated with molecular changes compatible with reduced NOS1 function. To assess the functional differences between S and AS hiPSC-CMs, we used the AP duration and I_{CaL} density since these were the two parameters mostly affected by NOS1 inhibition in GP-CMs.

3.2.1 Differences in the electrical activity between AS and S hiPSC-CMs

Membrane potential of hiPSC-CMs was recorded during pacing at 1 Hz in native and DC conditions (*Figure 5A* and *B*); AP parameters in the two conditions are summarized in Supplementary material online, *Table S3*. Membrane capacitance (C_m) was larger in S than in AS hiPSC-CMs (50.9 ± 4.8 vs. 37.2 ± 4.2 pF, P < 0.05). Diastolic membrane potential (E_{diast}) was around -40 mV in native conditions and approached -75 mV under DC; in both conditions, E_{diast} was similar between AS and S hiPSC-CMs (Supplementary material online, *Table S3*). In both native and DC conditions, APD_{90} was significantly longer (by 20.1% under DC) in S than in AS hiPSC-CMs (*Figure 5B*). Notably, albeit shortest in WT (with minor NOS1AP SNP) APD_{90} was not significantly prolonged in AS (major NOS1AP SNP) hiPSC-CMs (Supplementary material online, *Figure S6*); i.e. expression of the major *NOS1AP* allele partially countered the effect of KvLQT1 mutation on APD_{90}.

To verify whether such APD_{90} differences could be ascribed to abnormality of NOS1AP-dependent signalling, we tested the effect of NOS1AP siRNA and NOS1 inhibition (by SMTC) in WT hiPSC-CMs

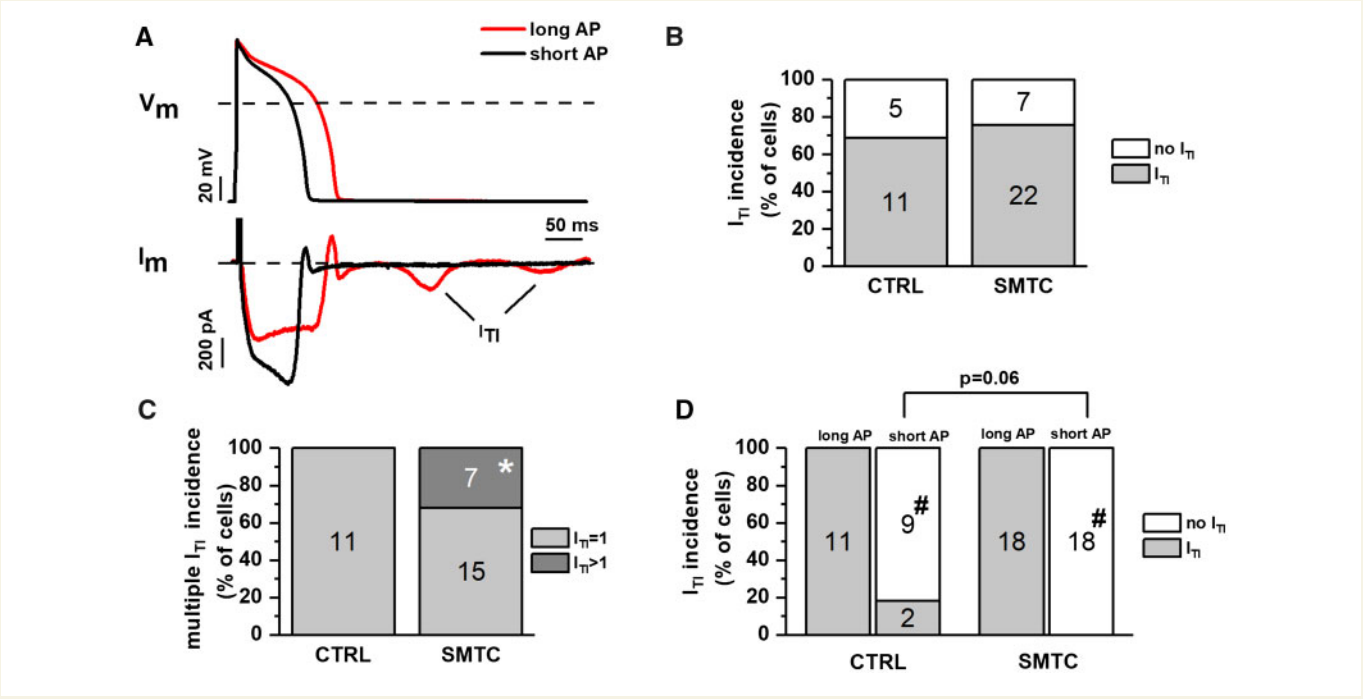

Figure 3 Interaction between NOS1 inhibition and APD in inducing I_{TI} events. I_{TI} events were induced by ISO 1 nM under AP clamp. (*A*) Representative membrane current recordings during long (APD_{90} = 140 ms, red) and short (APD_{90} = 100 ms, black) AP waveforms in the same myocyte; I_{TI} events are shown (arrows). (*B*) Percent of cells with no I_{TI} (white) or at least one I_{TI} (grey) event in CTRL and during NOS1 inhibition. (*C*) Percent of cells with one I_{TI} event (light grey) or >1 I_{TI} events (dark grey) in CTRL and during NOS1 inhibition. (*D*) Effect of APD shortening on I_{TI} incidence in CTRL and during NOS1 inhibition. Sample sizes: CTRL n = 16/3 and SMTC n = 29/6 for *B*; CTRL n = 11/3 and SMTC n = 22/6 for *C*; and CTRL n = 11/3 and SMTC n = 18/6 for *D*. $^{*}P < 0.05$ vs. CTRL. $^{\#}P < 0.05$ vs. long AP from the χ^2 test.

carrying the major *NOS1AP* SNP. Both the interventions prolonged APD_{90} (Supplementary material online, *Figure S7*).

ISO effect was tested by internal comparison in a subset of KvLQT1-mutant hiPSC-CMs under DC. ISO 1 nM failed to affect mean APD_{90} significantly in both S (ΔAPD: -2.7 ± 13.8%, NS) and AS (ΔAPD: -4.2 ± 15%, NS) hiPSC-CMs (*Figure 5C*), because of a high variability in the response. ISO 10 nM did not further modify APD_{90} in either group (data not shown).

EADs, DADs and triggered activity (*Figure 5D*) occurred (under DC conditions) in 18.2% (4/22) of AS hiPSC-CMs and in 46.15% (12/26) of S ($P < 0.05$; *Figure 5E*). Notably, both afterdepolarization types were often present within the same cell (e.g. rightmost panel in *Figure 5D*). APs containing EADs were not used for APD_{90} measurement.

3.2.2 Differences in I_{CaL} between AS and S hiPSC-CMs

Considering that the major effect of NOS1 inhibition in GP cardiomyocytes was I_{CaL} enhancement, a comparison of this current between S and AS hiPSC-CMs was particularly interesting for the purpose of this study; I_{CaL} parameters for the two experimental groups are reported in Supplementary material online, *Table S4*. Peak I_{CaL} density was significantly larger in S than in AS hiPSC-CMs at all potentials (*Figure 6A* and *B*), reflecting an increase in maximal normalized conductance *Figure 6C*. Accordingly, no differences were observed in I_{CaL} steady-state activation and inactivation curves (*Figure 6D* and Supplementary material online, *Table S4*).

3.2.3 Effect of NOS1 inhibition on intracellular Ca^{2+} dynamics in AS hiPSC-CMs

To test whether modulation of intracellular Ca^{2+} dynamics by endogenous NOS1 could be also observed in hiPSC-CMs, we applied SMTC to AS ones, i.e. those in which NOS1 signalling is expectedly intact (Supplementary material online, *Figure S8*). These experiments were performed under field-stimulation (un-patched cells) to avoid cytosol dialysis by the pipette solution. As for GP-CMs, SMTC effect on Ca^{2+} parameters was unexpectedly small and dispersed, achieving statistical significance only for slowing of Ca_T decay and increase in SR fractional Ca^{2+} release, suggestive of RyRs facilitation. As mentioned in Section 3.1.3, the small magnitude of the changes is likely the consequence of a measurement artefact. The results are detailed in the Supplementary material online.

3.2.4 Molecular characterization of hiPSC-CMs

The presence of the *KCNQ1*-A341V heterozygous mutation was confirmed in S and AS hiPSC-CMs.[13,14]

A first set of experiments aimed to test whether changes in NOS1AP and NOS1 expression and localization, compatible with loss of NOS1 function, could be detected in S hiPSC-CMs and, thus, ascribed to the minor variants of the *NOS1AP* SNPs.

NOS1AP signal was clearly detectable in hiPSC-CMs, in terms of transcript, protein levels (*Figure 7A*), and immunolocalization (*Figure 7B*). In AS hiPSC-CMs NOS1AP localization was cytosolic and roughly matched that of the sarcomeric protein cTnT (*Figure 7B*); though, it should be noticed that variable orientation of myofibrils and lack of T-

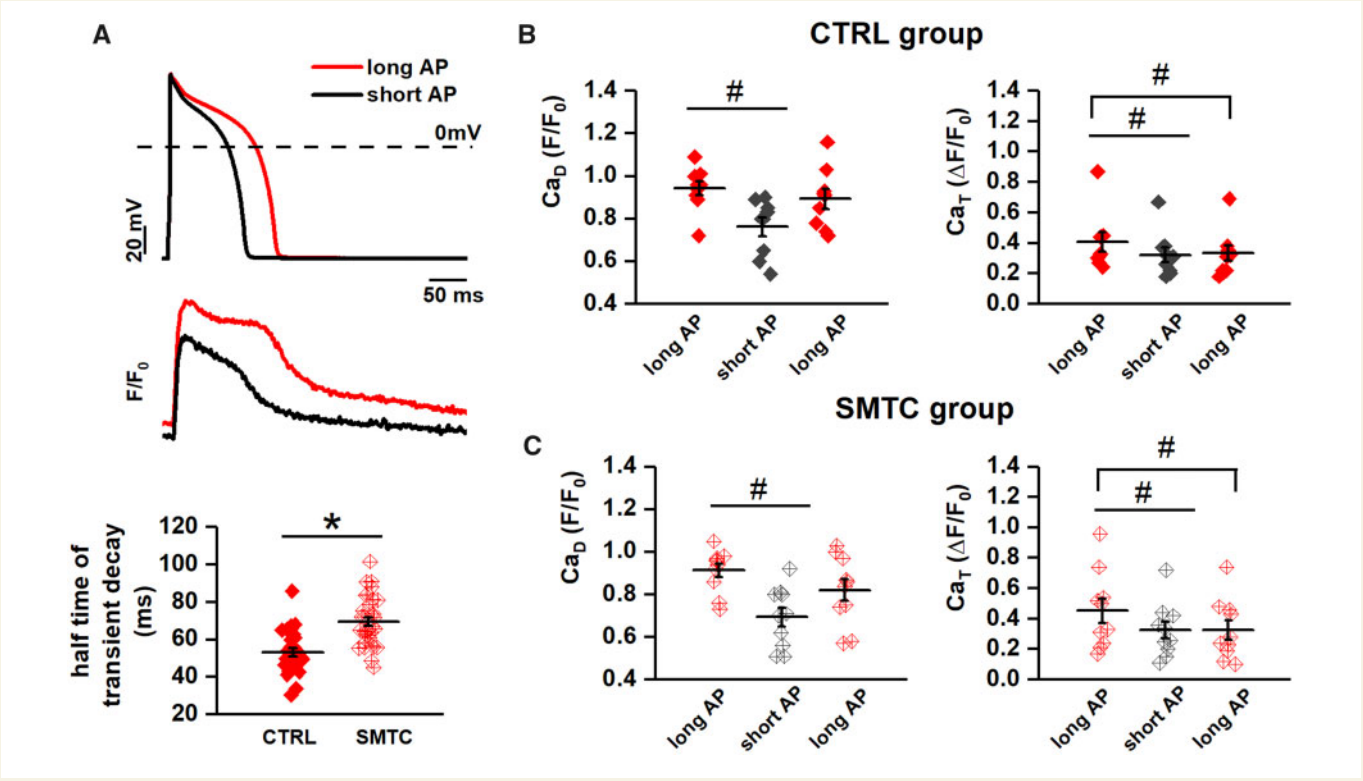

Figure 4 Interaction between NOS1 inhibition and APD in affecting intracellular Ca^{2+}. Cytosolic Ca^{2+} was measured under AP clamp with long and short APs in the presence of ISO 1 nM; long-short-long sequences were applied within each myocyte. (*A*) AP waveforms (top) and examples of the corresponding Ca^{2+} transients (bottom) recorded in CTRL. (*B*) Effect of APD on Ca_D (left) and Ca_T amplitude (right) in CTRL. (*C*) Half-time of Ca_T-decay in CTRL and during NOS1 inhibition. (*D*) Effect of APD on Ca_D and Ca_T amplitude during NOS1 inhibition. Sample sizes: CTRL $n = 10/4$ and SMCT $n = 9/3$ for *B*; CTRL $n = 29/10$ and SMTC $n = 34/9$ for *C*; CTRL $n = 10/4$ and SMCT $n = 9/3$ for *D*. $^{\#}P < 0.05$ vs. long AP. $^{*}P < 0.05$ vs. CTRL from the paired Student's *t*-test and two-way ANOVA for repeated measurements.

tubules periodicity make protein co-localization with intracellular structures difficult in hiPSC-CMs. In S hiPSC-CMs *NOS1AP* transcript and protein levels were sharply reduced (*Figure 7A*); lower NOS1AP expression in S than in AS hiPSC-CMs was also visible at immunostaining as a weaker cytosolic signal (*Figure 7B*).

NOS1 signal was strong in the nucleus and diffuse in the cytosol, where it roughly overlapped with that of cTnT and RyR2 (*Figure 7C* and Supplementary material online, *Figure S9*). NOS1 signal was lower, and its overlap with RyR2 weaker, in S than in AS hiPSC-CMs (Supplementary material online, *Figure S9*). Interaction between NOS1 and NOS1AP was investigated by the PLA, in which interacting proteins appear as intracellular bright dots. The intensity and amount of interaction dots were decreased in S hiPSC-CMs as compared to AS ones (*Figure 7D*). In the bottom panels of the figure, the interaction signal is overlapped with cTnT to show its relationship with cell structures.

A second set of experiments (reported in the Supplementary material online) aimed to test whether the influence of *NOS1AP* SNP could be generalized to WT hiPSC-CMs. To this end, we compared two WT hiPSC-CMs samples (one belonging to the SA population and the other not), which differed for the *NOS1AP* SNP variant (only r16, in this case). The results of NOS1AP and NOS1 immunolabelling (Supplementary material online, *Figures S10* and *S11*) match those obtained in LQT1 mutant cells, thus indicating that the effect of the r16 SNP variant on the expression and distribution of the two proteins is independent of the *KvLQT1* genotype.

4. Discussion

The main findings of this work can be summarized as follows. In a GP model of LQT1: (i) induction of marked SR instability by NOS1 inhibition was associated with enhancement of I_{CaL} and I_{NaL} and further APD prolongation; (ii) SR instability induced by NOS1 inhibition did not ensue if APD was kept constant and, once present, was suppressed by shortening APD (by AP clamp). In hiPSC-CMs, larger I_{CaL}, longer APD, and more afterdepolarizations differentiated S cells (minor *NOS1AP* allele) from AS ones (major *NOS1AP* allele); furthermore, the expression and co-localization of NOS1AP and NOS1 proteins were lower in S than in AS cells. The effects of NOS1 inhibition on intracellular Ca^{2+} dynamics were consistent with those on electrophysiology but of small magnitude; this was likely the consequence of Ca^{2+} buffering by the Ca^{2+}-sensitive dye.

4.1 Effect of NOS1 inhibition on APD and currents contributing to repolarization reserve

In GP-CMs, NOS1 inhibition markedly increased APD; this effect was at least similar to that of I_{Ks} blockade plus β-adrenergic stimulation and persisted when these factors were superimposed (*Figure 1*). Thus, defective NOS1 function may, by itself, delay repolarization, an effect adding to that of I_{Ks} deficiency, and β-adrenergic

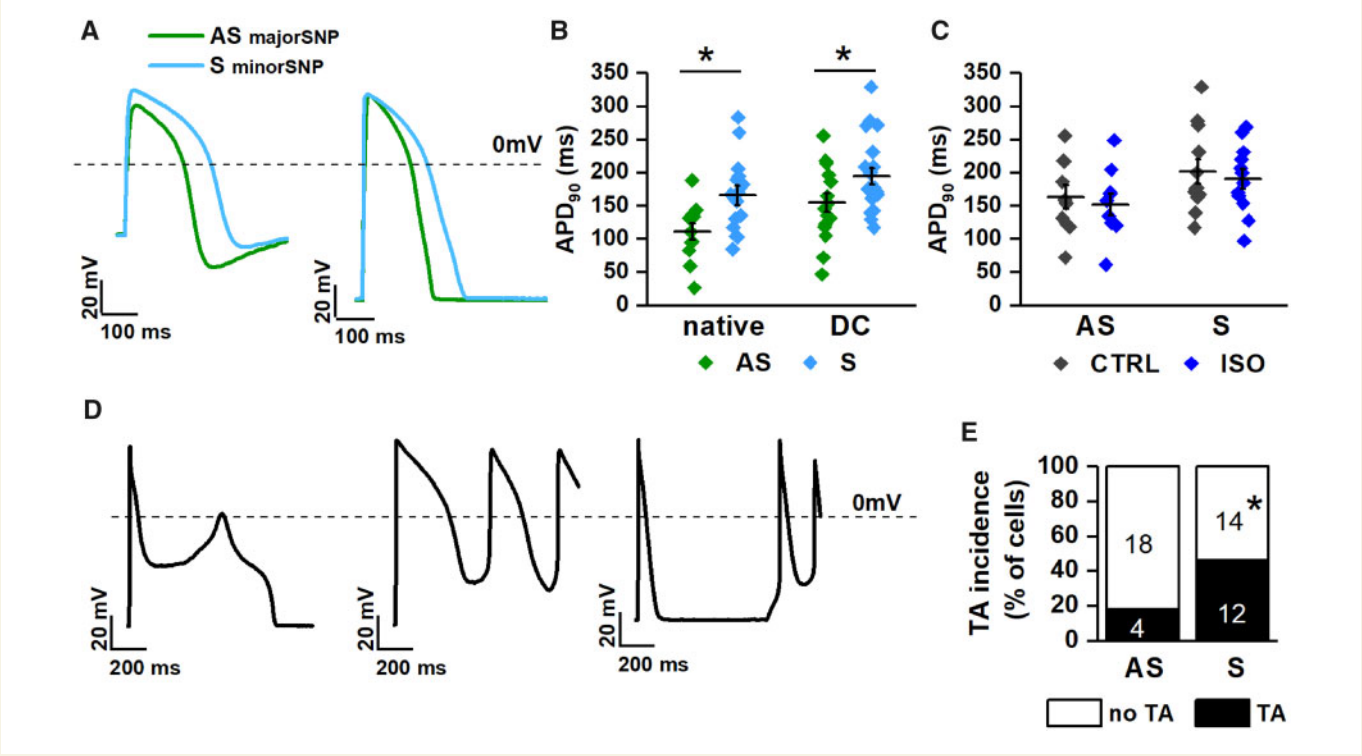

Figure 5 Comparison of electrical activity between AS and S hiPSC-CMs. (*A*) AP recordings in native (left) and DC (right) conditions; (*B*) APD_{90} in AS (green) vs. S (blue) hiPSC-CMs in native (left) and DC (right) conditions. (*C*) Effect of ISO (1 nM) on APD_{90} in AS vs. S hiPSC-CMs (DC condition). (*D*) Types of afterpotentials and trigger activity (TA) recorded in hiPSC-CMs. (*E*) Incidence of TA in AS vs. S hiPSC-CMs (DC condition). Sample sizes: AS nat $n = 12/6$ and S nat $n = 15/7$; AS DC $n = 16/6$ and S DC $n = 21/7$, for *B*; AS $n = 12/6$ and S $n = 16/7$ for *C*; AS $n = 22/6$ and S $n = 26/7$ for *E*. *$P < 0.05$ vs. AS from the unpaired Student's *t*-test and χ^2 test.

stimulation. Consistent with previous observations in NOS1$^{-/-}$ mice,[2,18] NOS1 inhibition increased I_{CaL} density (*Figure 2*), an effect attributed to tonic, cGMP-mediated, I_{CaL} inhibition by NO.[19] NOS1 inhibition also robustly enhanced I_{NaL}, an effect conceivably contributing to both APD prolongation and SR instability.[20] Previous work on Na^+ channel modulation by NO is controversial: both stimulation and inhibition are reported.[21] Notably, the present findings are the only concerning NOS1 activity specifically and the 'late' I_{Na} component.

The outward components of repolarization current (I_{Kr} and I_{Ks}) were not affected by NOS1 inhibition in a functionally significant way (Supplementary material online, *Figures S2* and *S3*). In previous work, NOS1AP overexpression, leading to increased NOS1 activity, slightly increased I_{Kr}.[22] Absence of I_{Kr} modulation by NOS1 inhibition (present study) suggests that the results of overexpression studies may not mirror those of inhibition of endogenous activity. Lack of NOS1 effect on I_{Ks} is consistent with the observation that I_{Ks} up-regulation is supported by NOS3 instead.[23]

I_{CaL} enhancement and APD prolongation would be expected to converge in causing EADs[24]; however, in GP-CMs, only DADs (also facilitated by I_{NaL} enhancement) were observed. Although EADs have been previously reported in this species, they usually occur at very low pacing rates; faster rates (as the 2 Hz used here) are known to favour DADs instead. Both EADs and DADs occurred in hiPSC-CMs, often within the same cell; since SCR events can also underlie EADs,[25] we speculate that, in the present setting, both types of afterpotentials may reflect SR instability.

4.2 Effect of NOS1 inhibition on SR stability

Under conditions relevant to arrhythmogenesis in LQT1 (I_{Ks} blockade and β-adrenergic stimulation), NOS1 inhibition (by two different agents) facilitated the occurrence of DADs, the arrhythmogenic epiphenomenon of SCR. At least two mechanisms may contribute to SCR facilitation by NOS1 inhibition in the present setting: (i) NOS1 activity may be required to support RyR2 nitrosylation,[4,15] a redox modification contributing to stabilize the channel in its closed state.[26] Lack of this action in the presence of adrenergic modulation of other membrane effectors (I_{CaL}, SERCA2a, etc.) may promote SCR during sympathetic activation; (ii) NOS1 inhibition directly enhanced I_{CaL}, I_{NaL} (*Figure 2*), and prolonged APD (*Figure 1*), thus conceivably changing the Ca^{2+} influx/efflux balance.[27] The increment in intracellular Ca^{2+}, potentially resulting from such changes, is a well-known factor in facilitation of SCR.[28] Operation of this mechanism is also suggested by shortening of the coupling between DADs and the preceding V-induced Ca^{2+} release (*Figure 1G*). Neuronal Na^+ channels, contributing to I_{NaL}, have been specifically implicated in linking APD prolongation to SCR facilitation.[29]

Intracellular Ca^{2+} measurements were carried out to directly evaluate the effect of NOS1 inhibition on intracellular Ca^{2+} handling. The low incidence of SCR events sharply contrasts with the high incidence of their electrical counterpart (DADs or I_{TI}) observed in experiments not requiring incubation with Fluo-4 AM. In isolated cardiomyocytes, DADs and I_{TI} events are invariably linked to Ca^{2+} waves and are often used as a readout of SCR. Therefore, the above discrepancy is likely the result of partial

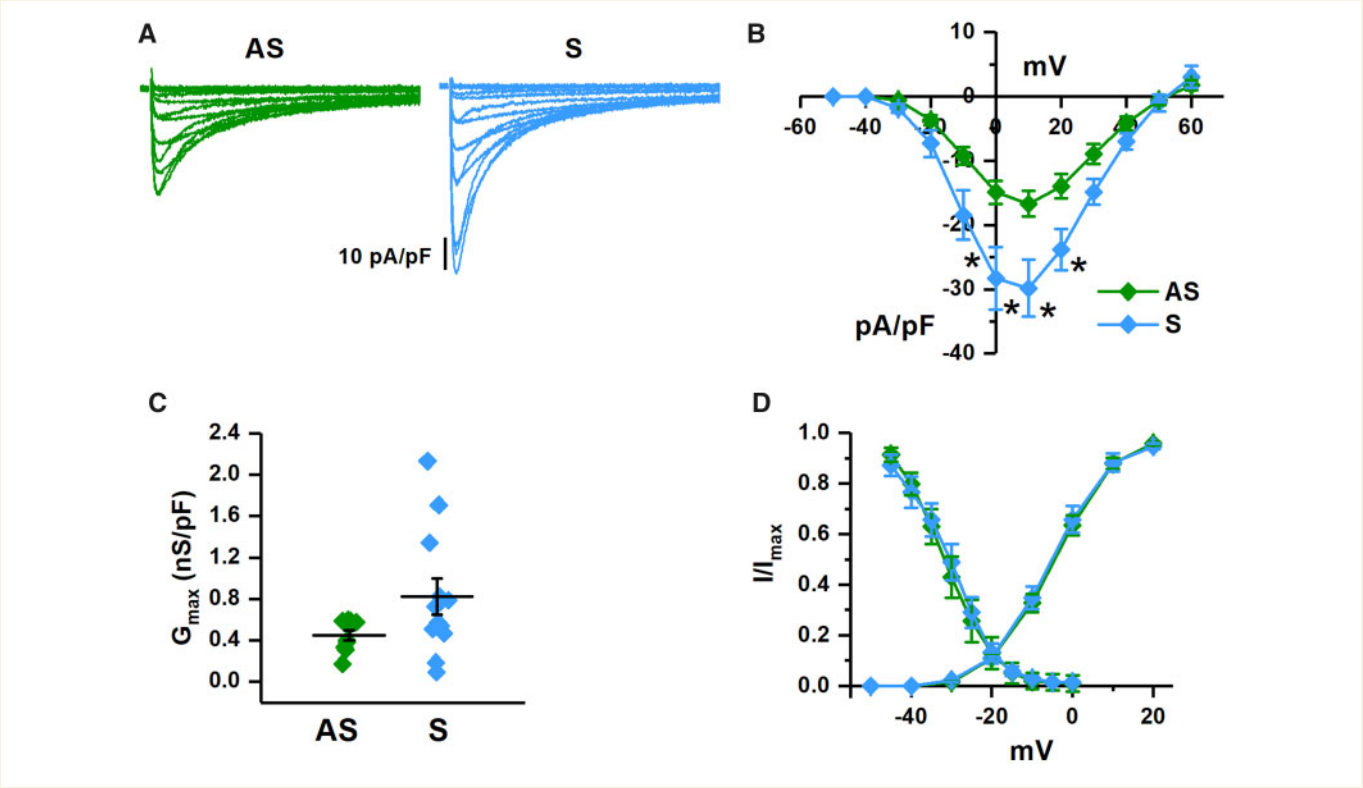

Figure 6 I_{CaL} properties in S vs. AS hiPSC-CMs. (*A*) Representative recordings of I_{CaL} at different voltages in AS (green) and S (blue) hiPSC-CMs. (*B*) Comparison of *I/V* relationships of peak I_{CaL} density. (*C*) Comparison of maximal I_{CaL} conductance (normalized for membrane capacity). (*D*) Comparison of steady-state activation and inactivation curves (AS $n = 10/3$ and S $n = 12/4$ for all panels). *$P < 0.05$ vs. AS from two-way ANOVA for repeated measurements.

Ca^{2+} buffering by Fluo-4 AM. Since also NOS1 activation depends on cytosolic Ca^{2+} levels,[30] Ca^{2+} buffering might have also minimized SMTC effect on Ca^{2+} handling. Fluo-4 impact on I_{TI} events, tested in preliminary experiments, support this view and suggests that Ca^{2+} recordings may underestimate SMTC effects; nonetheless, they were assessed anyway, to pursue at least a qualitative match with the electrophysiological effects.

Because SCR may deplete the SR, SMTC 'primary' effects on Ca^{2+} dynamics were assessed in their absence (GP experiments, Supplementary material online, *Figure S4B* and *C*). These effects, albeit small, are compatible with I_{CaL} enhancement (increased release trigger and Ca^{2+} influx) possibly balanced by a leakier SR. Indeed, SMTC increased tetracaine-sensitive Ca^{2+} leak (Supplementary material online, *Figure S4E*) and the resulting SR depletion (Supplementary material online, *Figure S4F*).

SMTC effect was even more elusive in AS hiPSC-CMs (Supplementary material online, *Figure S8*), but still compatible with RyRs facilitation (Supplementary material online, *Figure S8C* and *E*).

4.3 Interaction between NOS1 deficiency and APD prolongation in arrhythmogenesis and Ca^{2+} dynamics

The arrhythmogenic role acquired in LQT1 by otherwise inconsequential *NOS1AP* SNPs suggests that NOS1 deficiency and APD prolongation may converge to facilitate arrhythmogenic SCR. This hypothesis was addressed by imposing AP waveforms of different duration (AP clamp), i.e. in the absence of potentially contaminating pharmacological interventions. This involved clamping membrane potential; therefore, I_{TI} events were recorded, *in lieu* of DADs, to detect SCR. AP waveforms were selected to represent a 40% increase in APD starting from values normal for GP-CMs at 2 Hz; this change roughly matches that induced by NOS1 inhibition (*Figure 1*). Consistent and reversible abrogation of I_{TI} events by APD normalization (*Figure 3*) indicate that repolarization delay, such as that caused by *KCNQ1* mutations, can indeed lead to SCR in the context of NOS1 deficiency. A plausible mechanism for such an effect is change in the balance between Ca^{2+} influx (through I_{CaL}) and extrusion (by NCX) in each cycle, which may result in increased cell Ca^{2+} content.[27] In support of this interpretation, diastolic Ca^{2+} and Ca^{2+} transient amplitude decreased upon APD shortening (*Figure 4*). Even if SR Ca^{2+} accumulation may be limited by SCR events,[31] the larger Ca^{2+} transients amplitude suggests that APD changes did affect SR Ca^{2+} content. Unfortunately, the latter could not be estimated, because incomplete reversal of caffeine effect makes measurements before and after APD change unreliable.

In murine cardiomyocytes under field stimulation, *NOS1AP* silencing[32] or *NOS1* knockout[4] reduced Ca^{2+} transient amplitude and increased SR Ca^{2+} leak, an effect accounted for by reduced RyRs nitrosylation. In this study, albeit increasing I_{CaL}, NOS1 inhibition failed to affect diastolic Ca^{2+} or Ca^{2+} transient amplitude appreciably when APD was kept constant (AP clamp, *Figure 4B* and *D*) but increased them when APD was allowed to prolong (I clamp, Supplementary material online, *Figure S4*). On the other hand, as previously described, SMTC facilitated RyRs opening (Supplementary material online, *Figures S4E* and *F*) and SCR induction (Supplementary material online, *Figure S4G*). Thus, in determining the overall effect of NOS1 deficit, increased Ca^{2+} and Na^{+} influx may be

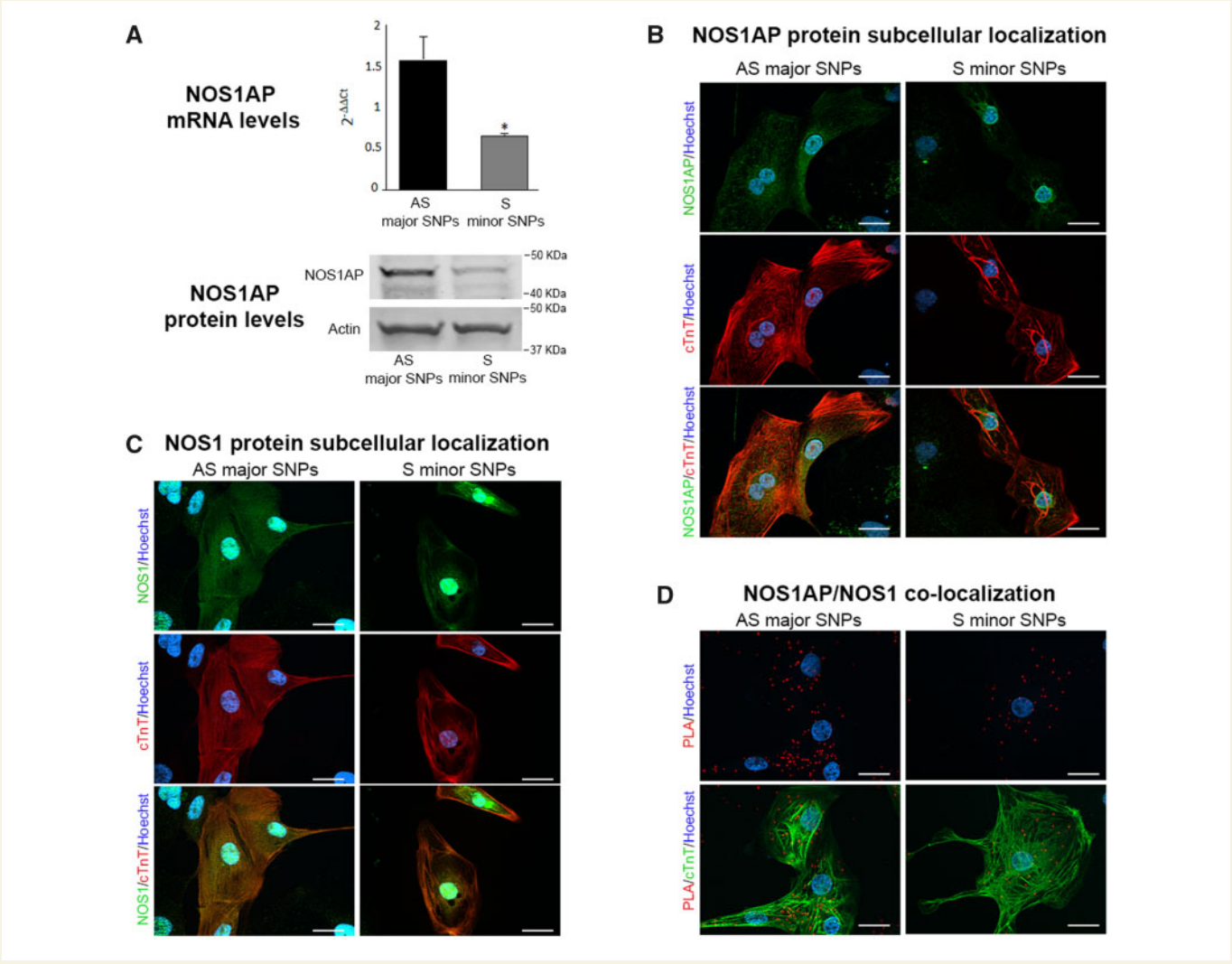

Figure 7 NOS1AP and NOS1 expression and localization in S vs. AS hiPSC-CMs. (*A*) comparison of NOS1AP transcript (top) and protein levels (bottom) between AS and S hiPSC-CMs (actin as loading control). (*B*) Immunostaining for NOS1AP protein (green) in AS and S hiPSC-CMs. (*C*) Immunostaining for NOS1 protein (green) in AS and S hiPSC-CMs. (*D*) NOS1AP/NOS interaction evaluated by the PLA, in AS and S hiPSC-CMs; interaction is revealed by bright red cytosolic dots. In *B* and *C*, the lower panels show the same field stained for the cardiac sarcomeric protein troponin T (cTnT, red) alone (middle) and in overlap (bottom); in *D*, PLA signals are overlapped with cTnT (bottom panel); nuclei in blue (Hoechst 33258). Scale bars = 20 μm. Sample size: AS $n = 6/3$ and S $n = 6/3$ for *A*. *$P < 0.01$ vs. AS from the unpaired Student's *t*-test.

offset by destabilization of the Ca^{2+} store. The findings also indicate that APD prolongation, also directly contributed by NOS1 dysfunction (I_{NaL} and I_{CaL} up-regulation), may be crucial in unveiling Ca^{2+} handling abnormality.

In conclusion, NOS1 deficiency may exaggerate APD prolongation caused by different mechanisms and act in concert with it to disrupt Ca^{2+} handling and facilitate arrhythmogenic SCR events.

4.4 Differences between AS and S hiPSC-CMs obtained from *KvLQT1* mutation carriers

Previous studies have shown that hiPSC-CMs recapitulate the typical features of LQTS associated with mutations affecting various proteins.[33,34] hiPSC-CMs were obtained from a large and well-characterized founder population[11]; this provides a unique opportunity to study the effect of modifiers with the lowest possible degree of confounding factors. Guided by the results obtained with NOS1 inhibition in GP-CMs, we chose to compare S and AS hiPSC-CMs for APD and I_{CaL} properties. Both cell types carried the same mutation on the *KVLQT1* gene but differed for the expression of *NOS1AP* variants (minor allele in S and major in AS); therefore, the observed differences are likely to reflect changes in NOS1AP expression/function.

APD was longer and I_{CaL} density was larger in S than in AS hiPSC-CMs (*Figures 5* and *6*), thus matching the effects of NOS1 inhibition in GP-CMs (*Figures 1* and *2*). The observation that *NOS1AP* SNPs may increase mortality even in users of dihydropyridine calcium channel blockers[35] might argue against a pathogenetic role of I_{CaL} enhancement. However, it should be considered that, at therapeutic concentrations, dihydropyrydines mainly block vascular I_{CaL}, with the resulting vasodilation reflexly triggering sympathetic activation.

β-adrenergic stimulation failed to shorten APD in both S and AS hiPSC-CMs, (*Figure 5C*). Although I_{Ks} was deficient (*KvLQT1* mutation) in both groups, we still expected S hiPSC-CMs to respond differently

because their I_{CaL} was larger. To this concern, it should be stressed that ISO effect was quite heterogeneous among hiPSC-CMs, which might have obscured differences between samples of necessarily small size.

NOS1 modulation of specific targets may be reduced by changes in protein expression or subcellular localization. In agreement with functional experiments, NOS1AP and NOS1 expression and co-localization with sarcomeric and SR proteins were reduced in S hiPSC-CMs (*Figure* 7). Furthermore, the PLA revealed reduced NOS1AP–NOS1 interaction in these cells (*Figure* 7*D*). This leads to the conclusion that the minor variant of *NOS1AP* gene may decrease NOS1AP expression, thus delocalizing NOS1 and reducing modulation of its compartment-specific targets.

The effect of *NOS1AP* variants associated with QT prolongation on NOS1AP expression is controversial. In previous work on GP-CMs, NOS1 and NOS1AP overexpression decreased I_{CaL} density and/or APD.[3,22,36] Our findings are in agreement with these observations; indeed, NOS1 inhibition (in GP and AS hiPSC-CMs) and NOS1AP down-regulation (in S hiPSC-CMs) increased I_{CaL} density and prolonged APD. Nonetheless, an opposite relationship between QT-prolonging *NOS1AP* SNPs and gene transcript (mRNA) was reported in two studies on human myocardial samples.[36,37] In these studies, the association between the SNPs and QT prolongation was merely correlative and rather weak[36]; furthermore, one of them[36] reported that, in contrast to what expected from the findings in human samples, NOS1AP overexpression in mammalian myocytes shortened APD. Also, at variance with results in mammalian myocytes, NOS1AP knock-down caused APD shortening in zebrafish,[38] but this may simply reflect the large species difference.

Our observation that the effect of *NOS1AP* r16 SNP on protein localization was also clearly detectable in WT hiPSC-CMs is consistent with the epidemiological notion that this gene variant is associated with longer repolarization and increased arrhythmia risk also in conditions other than LQT1.[7,35]

4.5 Limitations

A causative role of NOS1 dysfunction in I_{CaL} enhancement, APD prolongation, and SR instability of S hiPSC-CMs was inferred from the observation that the same effects were induced by NOS1 inhibition in GP-CMs. Correction of the *NOS1AP* gene variant, which would have lent further support to the conclusions, was not attempted because of limited availability of patient-derived hiPSC-CMs with the desired features. Nonetheless, full reproducibility in S hiPSC-CMs of the rather complex pattern of changes resulting from NOS1 inhibition in GP-CMs is unlikely a matter of chance.

The interaction between NOS1 deficiency and APD has been evaluated in 'acute' experiments. When repolarization is persistently prolonged, as in congenital LQTS, adaptive changes in the regulation of SR function may take place, thus potentially modifying the relationship between the electrical cycle and intracellular Ca^{2+} loading and/or the role of NOS1 signalling in SR stability.

Although NOS1 deficiency is more often reported to increase I_{CaL} (and, therefore, APD) in isolated cardiomyocytes, the direction of NOS1 modulation of I_{CaL} (and APD) might depend on the cell redox state, because of a change in the balance between channel S-nitrosylation and cGMP-regulated phosphorylation.[18] This suggests that redox state may be a further factor in the relationship between NOS1 function, prolonged repolarization, and arrhythmias.

The effect of NOS1 inhibition on intracellular Ca^{2+} is likely underestimated because of Ca^{2+} buffering by the dye; indeed, this may limit SCR occurrence and reduce the extent of NOS1 activity at baseline.

6. Conclusions and relevance

The present findings in GP-CMs suggest that loss of NOS1 function and APD prolongation converge to generate conditions of SR instability; this is likely to contribute to arrhythmogenesis in both congenital and acquired LQTS. They also indicate that NOS1 deficiency can, on its own, be a cause of prolonged repolarization, or contribute to the imbalance between inward and outward currents when primary ion channel abnormalities coexist. The results obtained in hiPSC-CMs are compatible with loss of NOS1 localization and function in cells from the S patient, carrying the minor *NOS1AP* variant. Taken together, our results support a cause–effect relationship between *NOS1AP* genotype, NOS1 function, and proarrhythmia. This is, of course, a step beyond the (merely correlative) demonstration of segregation of a genotype variant within a phenotype. The present results suggest that conditions leading to loss of NOS1 function (including, but not limited to *NOS1AP* SNPs) should be considered in the evaluation of the arrhythmogenic risk of prolonged repolarization syndromes in general. The results also point to I_{CaL} and I_{NaL} as potential therapeutic targets to minimize the aggravating role of the minor *NOS1AP* SNP under conditions of prolonged repolarization. The present findings contribute to the ongoing efforts to refine risk stratification in LQTS by the growing understanding of the impact, protective or damaging, of the genetic variants commonly referred to as 'modifier genes'.

Supplementary material

Supplementary material is available at *Cardiovascular Research* online.

Conflict of interest: none declared.

Funding

This work was supported by the Fondo Ricerca di Ateneo of Università Milano-Bicocca (2017-ATE-0206 to A.Z.), Ricerca Corrente of Fondazione IRCCS Policlinico San Matteo di Pavia (08064017 to M.G.) and Leducq Foundation ' (18CVD05 to M.G.). P.J.S. was supported by the National Institutes of Health (grant HL-68880), the Italian Ministry of Foreign Affairs and Leducq Foundation .

References

1. Beigi F, Oskouei BN, Zheng M, Cooke CA, Lamirault G, Hare JM. Cardiac nitric oxide synthase-1 localization within the cardiomyocyte is accompanied by the adaptor protein, CAPON. *Nitric Oxide* 2009;**21**:226–233.
2. Sears CE, Bryant SM, Ashley EA, Lygate CA, Rakovic S, Wallis HL, Neubauer S, Terrar DA, Casadei B. Cardiac neuronal nitric oxide synthase isoform regulates myocardial contraction and calcium handling. *Circ Res* 2003;**92**:e52–e59.
3. Burkard N, Rokita AG, Kaufmann SG, Hallhuber M, Wu R, Hu K, Hofmann U, Bonz A, Frantz S, Cartwright EJ, Neyses L, Maier LS, Maier SK, Renne T, Schuh K, Ritter O. Conditional neuronal nitric oxide synthase overexpression impairs myocardial contractility. *Circ Res* 2007;**100**:e32–e44.
4. Gonzalez DR, Beigi F, Treuer AV, Hare JM. Deficient ryanodine receptor S-nitrosylation increases sarcoplasmic reticulum calcium leak and arrhythmogenesis in cardiomyocytes. *Proc Natl Acad Sci U S A* 2007;**104**:20612–20617.
5. Zhang YH, Zhang MH, Sears CE, Emanuel K, Redwood C, El-Armouche A, Kranias EG, Casadei B. Reduced phospholamban phosphorylation is associated with impaired relaxation in left ventricular myocytes from neuronal NO synthase-deficient mice. *Circ Res* 2008;**102**:242–249.
6. Bencsik P, Kupai K, Giricz Z, Gorbe A, Huliak I, Furst S, Dux L, Csont T, Jancso G, Ferdinandy P. Cardiac capsaicin-sensitive sensory nerves regulate myocardial relaxation via S-nitrosylation of SERCA: role of peroxynitrite. *Br J Pharmacol* 2008;**153**:488–496.
7. Kao WHL, Arking DE, Post W, Rea TD, Sotoodehnia N, Prineas RJ, Bishe B, Doan BQ, Boerwinkle E, Psaty BM, Tomaselli GF, Coresh J, Siscovick DS, Marbán E, Spooner PM, Burke GL, Chakravarti A. Genetic variations in nitric oxide synthase 1

adaptor protein are associated with sudden cardiac death in US white community-based populations. *Circulation* 2009;**119**:940–951.
8. Crotti L, Monti MC, Insolia R, Peljto A, Goosen A, Brink PA, Greenberg DA, Schwartz PJ, George AL Jr. NOS1AP is a genetic modifier of the long-QT syndrome. *Circulation* 2009;**120**:1657–1663.
9. Tomas M, Napolitano C, De Giuli L, Bloise R, Subirana I, Malovini A, Bellazzi R, Arking DE, Marban E, Chakravarti A, Spooner PM, Priori SG. Polymorphisms in the NOS1AP gene modulate QT interval duration and risk of arrhythmias in the long QT syndrome. *J Am Coll Cardiol* 2010;**55**:2745–2752.
10. Schwartz PJ, Woosley RL. Predicting the Unpredictable: drug-Induced QT Prolongation and Torsades de Pointes. *J Am Coll Cardiol* 2016;**67**:1639–1650.
11. Brink PA, Crotti L, Corfield V, Goosen A, Durrheim G, Hedley P, Heradien M, Geldenhuys G, Vanoli E, Bacchini S, Spazzolini C, Lundquist AL, Roden DM, George AL, Jr, Schwartz PJ. Phenotypic variability and unusual clinical severity of congenital long-QT syndrome in a founder population. *Circulation* 2005;**112**:2602–2610.
12. Crotti L, Spazzolini C, Schwartz PJ, Shimizu W, Denjoy I, Schulze-Bahr E, Zaklyazminskaya EV, Swan H, Ackerman MJ, Moss AJ, Wilde AA, Horie M, Brink PA, Insolia R, De Ferrari GM, Crimi G. The common long-QT syndrome mutation KCNQ1/A341V causes unusually severe clinical manifestations in patients with different ethnic backgrounds: toward a mutation-specific risk stratification. *Circulation* 2007;**116**:2366–2375.
13. Mura M, Pisano F, Stefanello M, Ginevrino M, Boni M, Calabro F, Crotti L, Valente EM, Schwartz PJ, Brink PA, Gnecchi M. Generation of the human induced pluripotent stem cell (hiPSC) line PSMi007-A from a Long QT Syndrome type 1 patient carrier of two common variants in the NOS1AP gene. *Stem Cell Res* 2019;**36**:101416.
14. Mura M, Pisano F, Stefanello M, Ginevrino M, Boni M, Calabro F, Crotti L, Valente EM, Schwartz PJ, Brink PA, Gnecchi M. Generation of two human induced pluripotent stem cell (hiPSC) lines from a long QT syndrome South African founder population. *Stem Cell Res* 2019;**39**:101510.
15. Cutler MJ, Plummer BN, Wan X, Sun QA, Hess D, Liu H, Deschenes I, Rosenbaum DS, Stamler JS, Laurita KR. Aberrant S-nitrosylation mediates calcium-triggered ventricular arrhythmia in the intact heart. *Proc Natl Acad Sci U S A* 2012;**109**:18186–18191.
16. Wang Q, Curran ME, Splawski I, Burn TC, Millholland JM, VanRaay TJ, Shen J, Timothy KW, Vincent GM, de Jager T, Schwartz PJ, Towbin JA, Moss AJ, Atkinson DL, Landes GM, Connors TD, Keating MT. Positional cloning of a novel potassium channel gene: KVLQT1 mutations cause cardiac arrhythmias. *Nat Genet* 1996;**12**:17–23.
17. Schwartz PJ, Priori SG, Spazzolini C, Moss AJ, Vincent GM, Napolitano C, Denjoy I, Guicheney P, Breithardt G, Keating MT, Towbin JA, Beggs AH, Brink P, Wilde A, Toivonen L, Zareba W, Robinson JL, Timothy KW, Corfield V, Wattanasirichaigoon D, Corbett C, Haverkamp W, Schulze-Bahr E, Lehmann MH, Schwartz K, Coumel P, Bloise R. Genotype-phenotype correlation in the long-QT syndrome—gene-specific triggers for life-threatening arrhythmias. *Circulation* 2001;**103**:89–95.
18. Campbell DL, Stamler JS, Strauss HC. Redox modulation of L-type calcium channels in ferret ventricular myocytes. Dual mechanism regulation by nitric oxide and S-nitrosothiols. *J Gen Physiol* 1996;**108**:277–293.
19. Sumii K, Sperelakis N. cGMP-dependent protein kinase regulation of the L-type Ca2+ current in rat ventricular myocytes. *Circ Res* 1995;**77**:803–812.
20. Zaza A, Rocchetti M. The late Na+ current–origin and pathophysiological relevance. *Cardiovasc Drugs Ther* 2013;**27**:61–68.
21. Marionneau C, Abriel H. Regulation of the cardiac Na+ channel NaV1.5 by post-translational modifications. *J Mol Cell Cardiol* 2015;**82**:36–47.
22. Chang KC, Barth AS, Sasano T, Kizana E, Kashiwakura Y, Zhang Y, Foster DB, Marban E. CAPON modulates cardiac repolarization via neuronal nitric oxide synthase signaling in the heart. *Proc Natl Acad Sci U S A* 2008;**105**:4477–4482.
23. Bai CX, Namekata I, Kurokawa J, Tanaka H, Shigenobu K, Furukawa T. Role of nitric oxide in Ca2+ sensitivity of the slowly activating delayed rectifier K+ current in cardiac myocytes. *Circ Res* 2005;**96**:64–72.
24. January CT, Riddle JM. Early afterdepolarizations: mechanism of induction and block. A role for L-type Ca2+ current. *Circ Res* 1989;**64**:977–990.
25. Zhao Z, Wen H, Fefelova N, Allen C, Baba A, Matsuda T, Xie LH. Revisiting the ionic mechanisms of early afterdepolarizations in cardiomyocytes: predominant by Ca waves or Ca currents? *Am J Physiol Heart Circ Physiol* 2012;**302**:H1636–H1644.
26. Vielma AZ, Leon L, Fernandez IC, Gonzalez DR, Boric MP. Nitric oxide synthase 1 modulates basal and beta-adrenergic-stimulated contractility by rapid and reversible redox-dependent s-nitrosylation of the heart. *PLoS One* 2016;**11**:e0160813.
27. Bers DM. Cardiac excitation-contraction coupling. *Nature* 2002;**415**:198–205.
28. Stevens SCW, Terentyev D, Kalyanasundaram A, Periasamy M, Györke S. Intra-sarcoplasmic reticulum Ca2+ oscillations are driven by dynamic regulation of ryanodine receptor function by luminal Ca2+ in cardiomyocytes. *J Physiol* 2009;**587**:4863–4872.
29. Koleske M, Bonilla I, Thomas J, Zaman N, Baine S, Knollmann BC, Veeraraghavan R, Györke S, Radwański PB. Tetrodotoxin-sensitive Navs contribute to early and delayed afterdepolarizations in long QT arrhythmia models. *J Gen Physiol* 2018;**150**:991–1002.
30. Weissman BA, Jones CL, Liu Q, Gross SS. Activation and inactivation of neuronal nitric oxide synthase: characterization of Ca2+-dependent [125I]Calmodulin binding. *Eur J Pharmacol* 2002;**435**:9–18.
31. Venetucci LA, Trafford AW, Eisner DA. Increasing ryanodine receptor open probability alone does not produce arrhythmogenic calcium waves: threshold sarcoplasmic reticulum calcium content is required. *Circ Res* 2007;**100**:105–111.
32. Treuer AV, Gonzalez DR. NOS1AP modulates intracellular Ca(2+) in cardiac myocytes and is up-regulated in dystrophic cardiomyopathy. *Int J Physiol Pathophysiol Pharmacol* 2014;**6**:37–46.
33. Kiviaho AL, Ahola A, Larsson K, Penttinen K, Swan H, Pekkanen-Mattila M, Venalainen H, Paavola K, Hyttinen J, Aalto SK. Distinct electrophysiological and mechanical beating phenotypes of long QT syndrome type 1-specific cardiomyocytes carrying different mutations. *Int J Cardiol Heart Vasc* 2015;**8**:19–31.
34. Rocchetti M, Sala L, Dreizehnter L, Crotti L, Sinnecker D, Mura M, Pane LS, Altomare C, Torre E, Mostacciuolo G, Severi S, Porta A, De Ferrari GM, George AL Jr, Schwartz PJ, Gnecchi M, Moretti A, Zaza A. Elucidating arrhythmogenic mechanisms of long-QT syndrome CALM1-F142L mutation in patient-specific induced pluripotent stem cell-derived cardiomyocytes. *Cardiovasc Res* 2017;**113**:531–541.
35. Becker ML, Visser LE, Newton-Cheh C, Hofman A, Uitterlinden AG, Witteman JC, Stricker BH. A common NOS1AP genetic polymorphism is associated with increased cardiovascular mortality in users of dihydropyridine calcium channel blockers. *Br J Clin Pharmacol* 2009;**67**:61–67.
36. Kapoor A, Sekar RB, Hansen NF, Fox-Talbot K, Morley M, Pihur V, Chatterjee S, Brandimarto J, Moravec CS, Pulit SL, Consortium Q-I, Pfeufer A, Mullikin J, Ross M, Green ED, Bentley D, Newton-Cheh C, Boerwinkle E, Tomaselli GF, Cappola TP, Arking DE, Halushka MK, Chakravarti A. An enhancer polymorphism at the cardiomyocyte intercalated disc protein NOS1AP locus is a major regulator of the QT interval. *Am J Hum Genet* 2014;**94**:854–869.
37. Saba S, Mehdi H, Shah H, Islam Z, Aoun E, Termanini S, Mahjoub R, Aleong R, McTiernan CF, London B. Cardiac levels of NOS1AP RNA from right ventricular tissue recovered during lead extraction. *Heart Rhythm* 2012;**9**:399–404.
38. Milan DJ, Kim AM, Winterfield JR, Jones IL, Pfeufer A, Sanna S, Arking DE, Amsterdam AH, Sabeh KM, Mably JD, Rosenbaum DS, Peterson RT, Chakravarti A, KäÄB S, Roden DM, MacRae CA. Drug-sensitized zebrafish screen identifies multiple genes, including GINS3, as regulators of myocardial repolarization. *Circulation* 2009;**120**:553–559.